MOIST POTENTIAL VORTICITY DIAGNOSIS OF A MEIYU FRONTAL HEAVY RAIN PROCESS SIMULATION DURING SUMMER, 1991

Zhang Jing (张 晶),

Department of Geophysics, Peking University, Beijing 100871

Wei Tongjian (韦统健)

Department of Atmospheric Sciences, Nanjing University, Nanjing 210093

and *Zhang Xiangdong* (张向东)

Chinese Academy of Meteorological Sciences, Beijing 100081

Received April 10, 1994; revised April 20, 1995

ABSTRACT

In this paper, the heavy rain process from June 30 to July 2, 1991, has been simulated by MM4, and three-dimensional moist potential vorticity distribution of the simulation results has been calculated. It is shown that moist potential vorticity is an important physical variable to reveal heavy rain structure and dynamic mechanisms. Negative moist potential vorticity corresponds to the Meiyu front-wind shear line system and the negative center corresponds to the heavy rain center. Negative moist potential vorticity mainly attributes to the effects of meridional baroclinic term and convective unstable term. The former is favourable to the maintenance of zonal precipitation and the latter is the mechanism of the heavy rain center propagating along the rain belt. The heavy rain is contributed by the cooperative effects of conditional convective instability, baroclinic instability and upper air inertial instability.

Key words: moist potential vorticity, heavy rain, Meiyu, mesoscale model 4 (MM4)

I. INTRODUCTION

There occurred several heavy rain processes in the Changjiang-Huaihe region in 1991, which resulted in an unprecedented flood disaster. Therefore, the heavy rain study has been emphasized. However, the spacial and temporal scale of the heavy rain process is small and the regular data can not satisfy the needs of such mesoscale heavy rain studies. Consequently, the diagnosis of numerical simulation draws much more attention gradually (Zhang and Cho 1992). In this paper, the heavy rain process during 0000 GMT June 30 through 0000 GMT July 2, 1991, is analyzed on the basis of numerical simulation. The research has been developed on using moist potential vorticity (MPV) to discuss the moist symmetric stability of mesoscale weather systems in recent years. On the theoretical side, Hoskins (1974), Bennits and Hoskins (1979), Emanuel (1979) and Xu (1986) discussed two-dimensional moist symmetric stability. Negative MPV in the moisture atmosphere is correspondent to moist symmetric instability. Bennits and Hoskins (1979), as well as Reuter and Yau (1990), used

this theory to discuss the formation of the frontal rain belt structure and the mechanism of the rain belt development. Zhang and Cho (1992) explained MPV concept from two-dimensional to three-dimensional frame and studied the squall line structure. They successfully explained that the precipitation in the stratiform region behind the squall line was associated with the moist symmetric instability. In this paper, MPV of numerical simulation of weather process from June to July, 1991, will be analyzed and the dynamic structure and mechanism of the heavy rain process will be discussed. First, we will briefly introduce the numerical model MM4; second, analyze the weather pattern and the precipitation distribution of this heavy rain; third, dynamically analyze MPV of simulation results; and finally, discuss main conclusions.

II. MODEL DESCRIPTION

In this paper, the mesoscale numerical model MM4 is adopted for simulation. The model has the following main characteristics: The horizontal grid system adopts Arakawa B grids. Vertically, the model uses Sigma-coordinate and there are ten irregularly spaced levels. The top level is $p_t=100$ hPa. The horizontal grid spacing is 60 km. There are 41×40 grid points in the model area and the model center is located at 36°N, 117°E.

The main physical processes of model are as follows:

(1) Calculating surface temperature by use of surface heat balance equation.

(2) Using high resolution model to deal with planetary boundary condition.

(3) Adopting Kuo-Anthes cumulus convective parameterization scheme.

(4) Using time-dependent boundary condition as lateral boundary condition.

(5) Adopting horizontal and vertical diffusions.

The heavy rain process during June 30 through July 2 has been integrated for 48 hours by MM4 in this paper.

III. WEATHER PATTERN AND PRECIPITATION DISTRIBUTION

There existed the typical two blocking high circulation patterns, which is able to result in Meiyu, from 0000 GMT June 30 to 0000 GMT July 2, 1991. The two blocking highs embedded in westerly belt were located at the mid-Asia and the sea of Okhotsk, respectively. There appeared a low value system from Lake Baykal to the Bohai Gulf. The polar front area was obvious and the Pacific subtropical high penetrated into the South China region. The surface cyclone-cold front system, originally situated from Mongolia, North China to the northern part of Sichuan Province, migrated gradually southeastward. Up to and after 0000 GMT July 1, the above mentioned system arrived in the areas from the Japan Sea to the mid and low reaches of the Changjiang River and became a quasi-stationary front. Later on, the western part of the quasi-stationary front weakened. Corresponding to the surface quasi-stationary front, there existed a Changjiang-Huaihe wind shear line system in the mid and low troposphere. The precipitation appeared between the quasi-stationary front and the wind shear line and assumed zonal distribution.

MM4 successfully simulated above weather system distributions and evolution processes (figures neglected). Therefore, the model outputs provide spatial and temporal intensive density and dynamically coherent data set for diagnoses. The simulated precipitation is close to

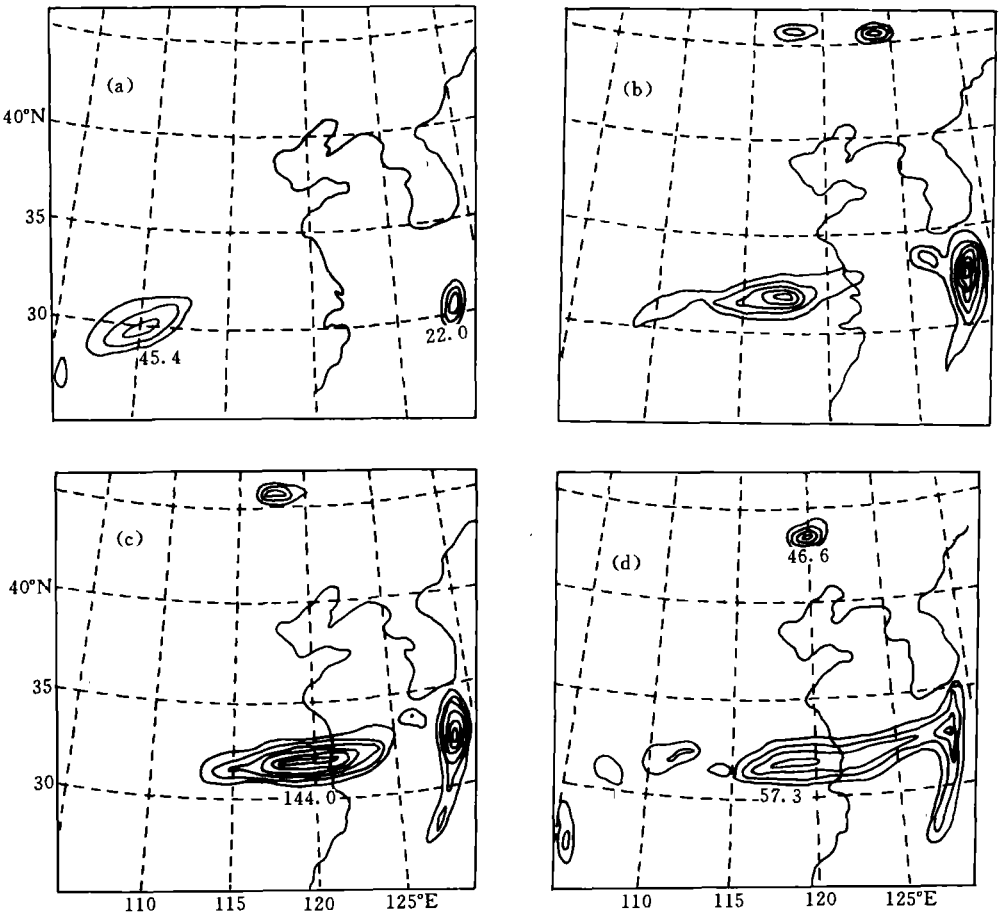

Fig. 1. The simulated precipitation distributions every 12 hours from 0000 GMT June 30 to 0000 GMT July 2 (unit: mm).

the observed one (figures neglected). The centers of both simulated and observed precipitations are approximately consistent except that the simulated precipitation is less than the observed one. Figure 1 gives the simulated precipitation distributions every 12 hours. It can be seen that the precipitation center is situated in the southwest area of China (i. e. 30°N, 110°E). After July 1, it weakened. From July 1 to July 2, there occurred two heavy rain processes in the Changjiang-Huaihe region. The first one originally appeared to the east of the Dabie Mountains at 0000 GMT July 1 and then moved eastward gradually. It was along the coast at 1200 GMT July 1. The precipitation amount every 12 hours is more than 100 mm, a very heavy rain process. The second one originally appeared in the Dabie Mountains region and then moved eastward. It was near 120°E at 0000 GMT July 2. The precipitation amount every 12 hours was between 60 mm and 100 mm.

IV. MPV STRUCTURE AND DYNAMIC MECHANISM OF HEAVY RAIN SYSTEMS

1. *Calculation Method of MPV*

Three-dimensional MPV in the z-coordinate is expressed as

$$MPV = \frac{1}{\rho}\left\{\frac{\partial \theta_e}{\partial x}\left(\frac{\partial w}{\partial y} - \frac{\partial v}{\partial z}\right) + \frac{\partial \theta_e}{\partial y}\left(\frac{\partial u}{\partial z} - \frac{\partial w}{\partial x}\right) + \frac{\partial \theta_e}{\partial z}\left(\frac{\partial v}{\partial x} - \frac{\partial u}{\partial y} + f\right)\right\}, \quad (1)$$

where u, v and w are wind components in x, y and z directions respectively. ρ is air density. θ_e is equivalent potential temperature and f is Coriolis parameter. The former two terms of right side of above formula represent the contributions of atmospheric baroclinity. The third term represents the contributions of convective stability and inertial stability. The calculation results show that the value of the third term is the largest. Therefore, the negative correlation between $\partial \theta_e/\partial z$ and $[(\partial v/\partial x) - (\partial u/\partial y) + f]$ can result in negative MPV, that is to say, there occurs symmetric instability. Usually, we use potential temperature in place of equivalent potential temperature in MPV, and can obtain Ertel potential vorticity. Ertel potential vorticity is conservative in the inviscid and adiabatic atmosphere. However, in the moisture atmosphere, MPV is conserved only under saturation condition or in the two-dimensional frame. Zhang and Cho (1992) simulated a squall line process using MM4 and calculated its MPV. Sinks and sources give rise to the non-conservation of MPV. These sinks and sources include numerical diffusion, condensation and melting, liquid water content, as well as convection and turbulence parameterizations, etc. But, Zhang and Cho (1992) indicate that these sinks and sources are secondary to MPV, while the effects of the resolvable scale squall line circulation are predominant. These calculation results are consistent with observation analyses. Consequently, to some degree, MPV can be considered as a quasi-conservative variable in discussing the appearance and development of dynamic instability. The calculations in this paper further show that MPV structure is predominantly determined by the heavy rain system circulations and then verify the above statement. Next, we will introduce the calculation method of MPV.

First, the outputs of MM4 are interpolated into the Z-coordinate. And then MPV is calculated using difference method. In order to get rid of the lateral boundary effects, five-cycle grid values near the lateral boundary in the outputs have been removed. The grid points change from 41×40 to 31×30. The calculation domain is 28°N—43°N, 107°E—127°E and the grid spacing is 60 km. Because of topographic effect and calculation ability, irregular interval 19 levels are adopted vertically, with 200 m from levels 1 to 6, 500 m from levels 6 to 10 and 1000 m from levels 10 to 19. Therefore, three-dimensional MPV can be calculated.

2. *Horizontal Structure of MPV*

Figure 2 gives MPV horizontal distribution. In the low level, at 0000 GMT June 30, MPV was negative over a large part of China. A negative MPV belt, with three centers in the Inner Mongolia, North China and the Southwest China respectively, was located behind the surface cold front. This indicates that the cold front system assumed very strong negative MPV structure in the lower atmosphere. The negative center in the Southwest China corresponded to the Southwest vortex and the surface inverted trough, while a large area of positive MPV just corresponded to the subtropical high. The low level MPV distribution reflected well the allocations of the low level weather systems. At 1200 GMT June 30 (figure neglected), the MPV center in the Southwest region had nearly no movement. But its intensity obviously increased. Correspondently, there occurred a more intensive precipitation process in this region (Fig. 1a). Afterwords, the cyclone-cold front system moved southward

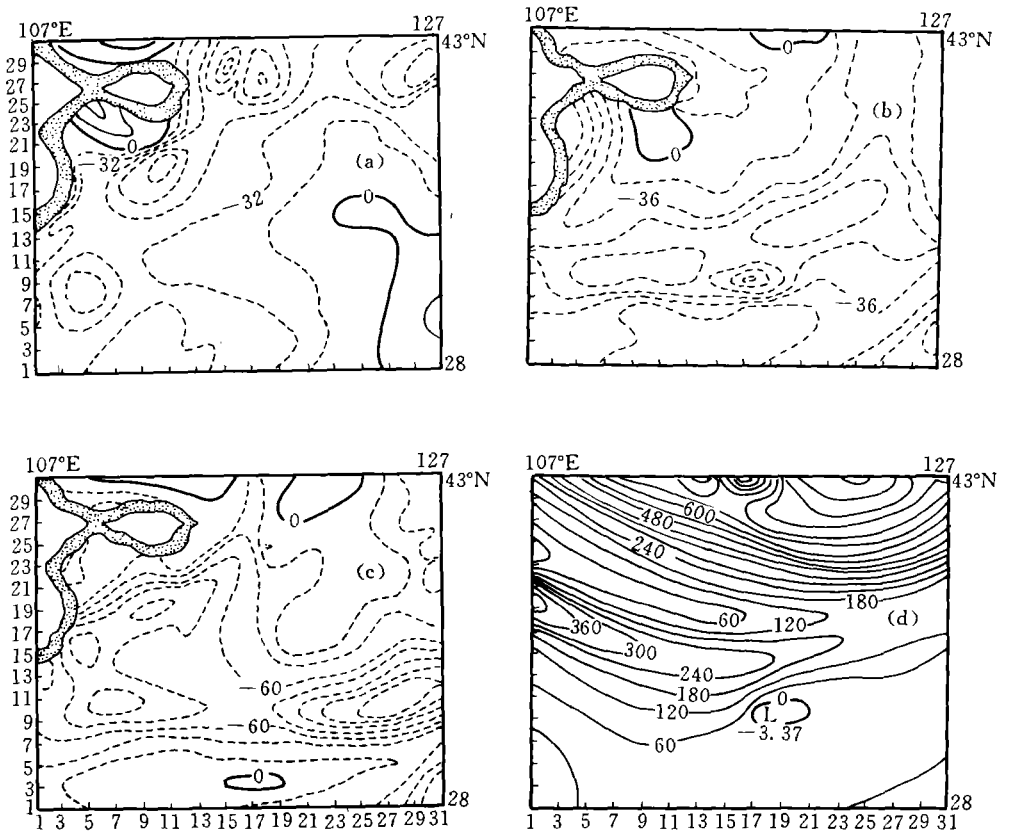

Fig. 2. (a) — (c) MPV distributions every 24 hours at 1500 m from 0000 GMT June 30 to 0000 GMT July 2. (d) MPV distribution at 11000 m on 0000 GMT July 1. Solid line: $\geqslant 0$; dashed line: < 0 (unit: $10^{-8}\ m^2\ k\ s^{-1}\ kg^{-1}$).

and became stationary gradually in the Changjiang-Huaihe region at 0000 GMT July 1. Associated with the cold front, the negative belt maintained its state and also propagated southward. At 0000 GMT July 1, the negative MPV belt with east-west orientation was located in the Changjiang-Huaihe region. Therefore, the cold front which propagated southward brought about a large amount of negative MPV and resulted in a large negative MPV belt in the Changjiang-Huaihe region. At 0000 GMT July 1 (Fig. 2b), there appeared a strong center in the negative MPV belt, (i.e. 32°N, 118°E). This center was correspondent to the strongest precipitation in the Changjiang River valley (Fig. 1b). At 1200 GMT July 1 (figure neglected), this negative center shifted eastward, and, correspondingly, the heavy rain center also shifted to the coast of the East China. Both positions were completely consistent. Similar to this process, the other negative MPV center formed when the above mentioned center shifted to the coast. The new center gave rise to the second heavy rain center, and moved at 32°N, 125°E at 0000 GMT July 2. Accordingly, it can be seen that the negative MPV belt in the low level reflects well the low level Meiyu front-wind shear line system, while the strong negative center embedded in the belt always corresponds to the heavy rain center. This suggests that negative MPV is an important mechanism triggering heavy rain processes.

The upper level three-dimensional MPV distribution is completely consistent with the upper level jet distribution (figure neglected) (Wei and Zhang 1995). At 0000 GMT June 30 (figure neglected), positive MPV prevailed over the whole grid domain and assumed zonal distribution. Later on, with the upper level jet splitting into the southern and the northern branches, there alternatively appeared three large and small zonal regions of MPV along the jet orientation to the north of 35°N (Fig. 2d). The northern large value region corresponded to the positive shear vorticity region of the northern jet, while the southern large value region corresponded to that of the southern jet. The small value region between the above two large value regions corresponded to the negative shear vorticity belt between the northern jet and the upper level small wind area. In addition, there appeared a small area of negative MPV near 32°N, 118°E, which corresponded to the strong rainfall center at 0000 GMT July 1. This attributes to the intensive convective vertical transport which brought the low level negative MPV center up to the upper level (Fig. 2b).

Figure 3 depicts the distributions of each term of MPV in the lower atmosphere. It can be seen generally that the MPV distribution is primarily consistent with the distribution of the third term $(MPV)_z$. That is to say, the negative MPV center is predominantly contributed by convective stability and absolute vertical vorticity. But, according to Figs. 3b—3d, it can be seen that the contribution of the second term $(MPV)_y$ to the negative MPV belt can not be neglected and it sometimes has the same order as the third term. As well known, the north cold front has very strong baroclinity. The meridional gradient of equivalent potential temperature is very large, and the second term of MPV describes this character. The contribution of the first term, describing zonal baroclinity, is the smallest (Fig. 3a). We will further analyze the last term of MPV as follows. AT 0000 GMT June 30, the third term $(MPV)_z$ had three negative centers situated in the Southwest region, the North China and the Inner Mongolia, which were the same as the positions of three negative MPV centers shown in Fig. 2a. At this time, the value of $(MPV)_y$ is smaller (Fig. 3b). At 1200 GMT June 30 (figure neglected), the negative $(MPV)_z$ center which was originally situated in the Inner Mongolia moved eastward, the negative $(MPV)_z$ center which was situated in the North China weakened and the negative $(MPV)_z$ center which was situated in the Southwest region further intensifies. These were completely consistent with negative MPV intensification in the Southwest region and occurrence of a heavy rain process. In the meantime, $(MPV)_y$ also intensified and formed a little strong negative center in Shandong Province. The composition of the distributions of $(MPV)_z$ and $(MPV)_y$ was similar to MPV distribution. After 0000 GMT July 1, the orders of magnitude of both $(MPV)_y$ and $(MPV)_z$ were about the same, i.e., the contributions of both terms were equivalent. Along the quasi-stationary front-wind shear line, $(MPV)_y$ produced a strong negative $(MPV)_y$ belt with a east-west orientation in the Changjiang-Huaihe region. The structure of the belt was more uniform. This reflects that the meridional moisture baroclinity continuously intensified and maintained when the cold front migrated southward and became the Changjiang-Huaihe quasi-stationary front. Obviously after 0000 GMT July 1, the strong negative MPV belt in the Changjiang-Huaihe region dominantly resulted from the contribution of the cold front moisture baroclinity. After 0000 GMT July 1, there appeared a strong negative MPV center and a heavy rainfall. Compared Figs. 2b and 2c with Figs. 3f and 3g, these strong negative MPV centers dominantly result from the

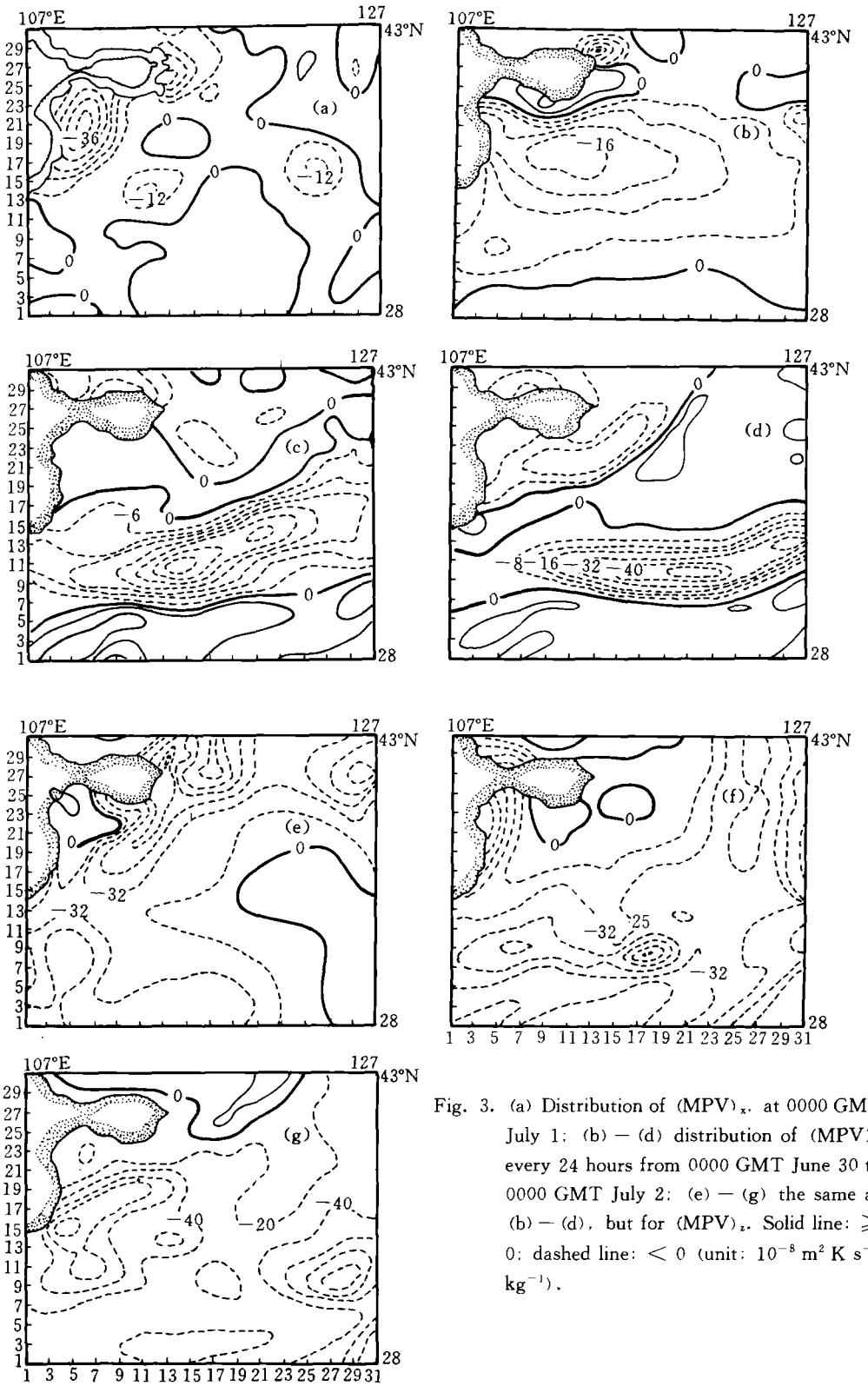

Fig. 3. (a) Distribution of $(MPV)_x$ at 0000 GMT July 1; (b) — (d) distribution of $(MPV)_y$ every 24 hours from 0000 GMT June 30 to 0000 GMT July 2; (e) — (g) the same as (b) — (d), but for $(MPV)_z$. Solid line: $\geqslant 0$; dashed line: < 0 (unit: 10^{-8} m^2 K s^{-1} kg^{-1}).

contribution of $(MPV)_z$, i. e., the contributions of both convective stability and absolute vertical vorticity, which resulted in two strong negative MPV centers in the Dabie Mountains twice. These centers then propagated eastward and resulted in two heavy rain processes in the eastern region.

According to above analyses, in this heavy rain process, although the rain belt from the Southwest region to the Changjiang-Huaihe region exhibits negative MPV structure, the dynamic causes of heavy rainfalls, negative MPV and their weather systems in the eastern part and the western part of the rain belt are different. The weather system of the western heavy rain belongs to the subtropical system, and the rainfall results from the Southwest vortex. In terms of contributions of each term of MPV, the negative MPV in Southwest vortex is resulted in by $(MPV)_z$, i. e., the convective activities and the cyclonic structure. The eastern heavy rain belongs to the front system, which is the quasi-stationary front-wind shear line system produced by the confrontation between the southeastward propagating cold high and the subtropical high. According to the contributions of each term of MPV, the contributions of $(MPV)_y$ and $(MPV)_z$ are equivalent for the eastern front heavy rain systems. $(MPV)_y$, the meridional moisture baroclinic effect, constitutes the zonal structure of negative MPV with a east-west orientation and cooperates with the front rain belt. The negative MPV center produced by $(MPV)_z$ embedded in this structure exhibits obvious eastward moving feature. These are dynamical mechanisms responsible for the large-scale front rain belt and the embedded mobile heavy rain. Therefore, the precipitation in the eastern region not only results from convective activity but also is affected by the effects of moisture baroclinity.

In order to better understand moisture potential vorticity structure of the heavy rain processes, we will analyze the vertical structure of MPV in the following section.

3. *Vertical Structure of MPV*

Strong precipitation occurred in the western part of the rain belt on June 30. Figure 4a depicts the meridional vertical section of MPV along the western heavy rain center, i. e., 110°E at 1200 GMT June 30. At 0000 GMT June 30, negative MPV appeared in the south low level in the section, and positive MPV appeared in the north upper level. The zero line of MPV appeared in about 4000 m (figure neglected). At 1200 GMT June 30 (Fig. 4a), MPV changed into negative value over the whole low part of the section. The negative center in the Southwest region obviously intensified. In terms of vertical velocity distribution (figure neglected), there was strong upward motion in this position. At this time, the rainfall was about 100 mm per six hours. According to above analyses, the negative MPV center mainly attributes to the contribution of the third term $(MPV)_z$. It is no doubt that this precipitation is convective one. After the calculation of two factors of $(MPV)_z$—absolute vertical vorticity and equivalent potential temperature it is found that there was a positive vorticity center in the low troposphere and the intensity reached the strongest at 1200 GMT June 30. Also, in this region, there existed conditional unstable area (figure neglected). But in terms of Fig. 4a, this convective activity only occurred below 500 m and did not develop up to the upper level to make a protruding negative area. This may be the reason of small precipitation in this region.

Figures 4b and 4c are MPV meridional-vertical sections along the eastern heavy rain center, i. e., 118°E. It went through the heavy rain center at 0000 GMT July 1 and was close to the second heavy rain center at 0000 GMT July 2 (refer to Figs. 2b and 2c or Figs. 1b and 1d). At 0000 GMT June 30 (figure neglected), the zero line of MPV was in the mid level and separated the troposphere into the positive and the negative areas. The positive and the negative centers were located at about 40°N ($y=24$). At 0000 GMT and 1200 GMT June 30 (figure neglected), the upper and the low level patterns had no obvious changes. At 1800 GMT (figure neglected), there was a negative MPV center (-95.7) in the low level, which first appeared at 35°N ($y=15$). At 0000 GMT July 1 (Fig. 4b), there appeared another stronger negative center, which had MPV zero isoline protruded to 12 000 m. A very narrow negative MPV area penetrated the whole troposphere. Because of the quasi-conservation of MPV, these imply that intensive convection took place. Simultaneously, downward movement produced to the north of the strong upward movement area, which had MPV zero isoline descended from 4000 m to 1600 m and caused the upper level positive MPV transport downward. According to the vertical velocity distribution at this time (figure neglected), there was a narrow and strong upward motion area corresponding to the upward transportation of negative MPV in the convective area. After this time, a strong negative MPV center maintained in the low troposphere within the range of about 31°N—34°N from 0000 GMT to 1800 GMT July 1. But the zero isoline still kept horizontal. This is the reflection of the quasi-stationary front moisture baroclinity. At 0000 GMT July 2, another strong convection took place (Fig. 4c). Its situation is the same as that shown in Fig. 4b.

In order to study the effects of $(MPV)_y$ and $(MPV)_z$ on the heavy rain, Figure 5 gives the meridional sections of $(MPV)_y$ and $(MPV)_z$ along 118°E ($x=19$) at 0000 GMT July 1. It

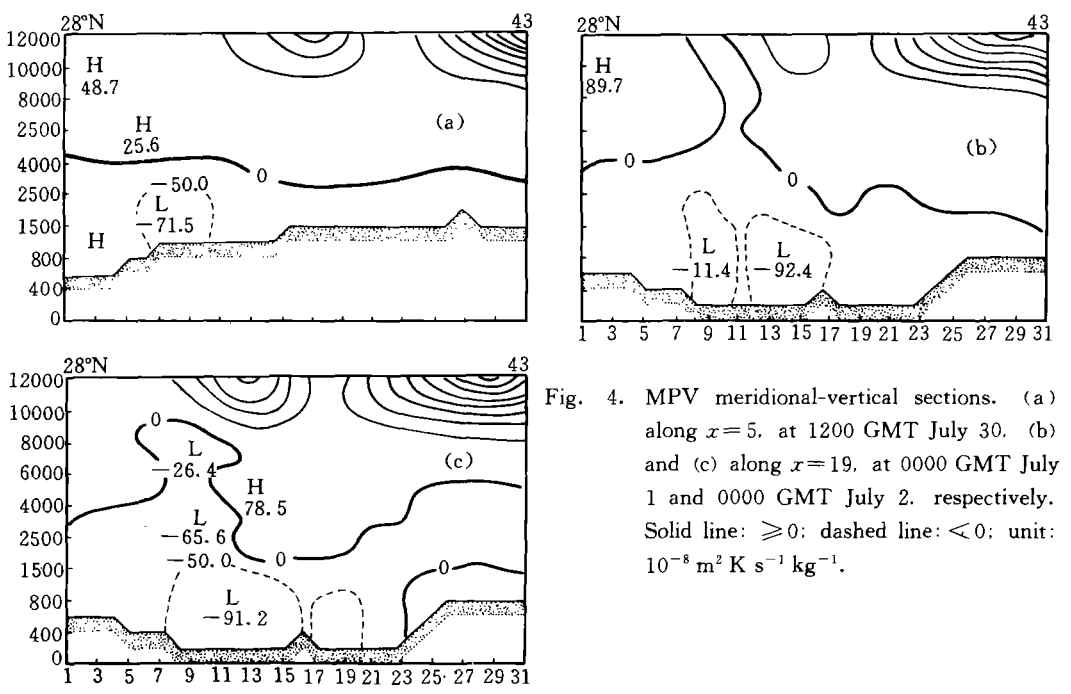

Fig. 4. MPV meridional-vertical sections. (a) along $x=5$, at 1200 GMT July 30. (b) and (c) along $x=19$, at 0000 GMT July 1 and 0000 GMT July 2, respectively. Solid line: $\geqslant 0$; dashed line: <0; unit: $10^{-8}\ m^2\ K\ s^{-1}\ kg^{-1}$.

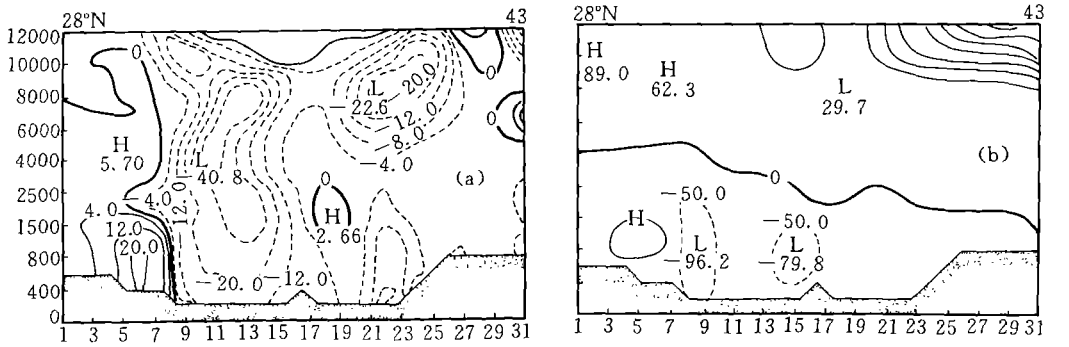

Fig. 5. $(MPV)_y$ and $(MPV)_z$ meridional sections along $x=19$ at 0000 GMT July 1, respectively in (a) and (b). Solid line: $\geqslant 0$; dashed line: <0; unit: $10^{-8}\ m^2\ K\ s^{-1}kg^{-1}$.

can be seen that, below 1500 m, the contribution of $(MPV)_z$ to negative MPV is dominant and the contribution of $(MPV)_y$ is very small. In the mid level between 1500 m—4000 m, the contributions of two terms are almost equal. Above 4000 m, the contribution of $(MPV)_y$ shows dominant importance. These indicate that the front baroclinic effects are important factors to bring about the heavy rain in the Changjiang-Huaihe region. According to the absolute vorticity distribution in the same section (figure neglected), there is a narrow strong positive absolute vorticity center in 10000 m. The equivalent potential temperature distribution in this section (figure neglected) shows that there exist the strongest conditional convective unstable stratification below 4000 m and the stable stratification corresponding to the upper level negative vorticity. Consequently, in the mid and low tropospheres, the intensive convective instability and the intensive positive absolute vertical vorticity give rise to a strong negative MPV center; in the upper troposphere, the inertial instability, caused by the upper level jet (Wei and Zhang 1995), cooperating stable stratification, contributes to negative MPV. Here, the MPV vertical structure further demonstrates that the heavy rain in the Changjiang-Huaihe region differs from that in the western region. The heavy rain in the western region mainly attributes to the convective unstable effect in the low troposphere, while the heavy rain in the Changjiang-Huaihe region mainly attributes to the cooperation of the convective instability and the frontal meridional baroclinic effect in the low troposphere. To some extent, the inertial instability to the south of the upper level jet also plays a certain role.

It can be found from the evolution of every variables that, in the Changjiang-Huaihe region at 0000 GMT July 1, the reasons of strong negative MPV center and the heavy rain taking place abruptly are: first, the front, arriving in the Changjiang-Huaihe region at 0000 GMT July 1, bringing about strong negative MPV zonal belt; second, the absolute vertical vorticity abruptly increasing. Before 0000 GMT July 1, a convective unstable area maintained in the mid and lower troposphere in the Changjiang-Huaihe region. Its variation was small. But, from 0000 GMT June 30 to 0000 GMT July 1, the absolute vertical vorticity increased about ten times (from 9.84×10^{-6} to $87.65\times10^{-6}\ s^{-1}$) so that the strong negative MPV center formed. The vorticity increasing is related to the acceleration of the southwest jet. The acceleration of the jet produced an intensive positive shear vorticity area to the north (Wei and Zhang 1995). After 0000 GMT July 1, the negative MPV weakened and the rainfall

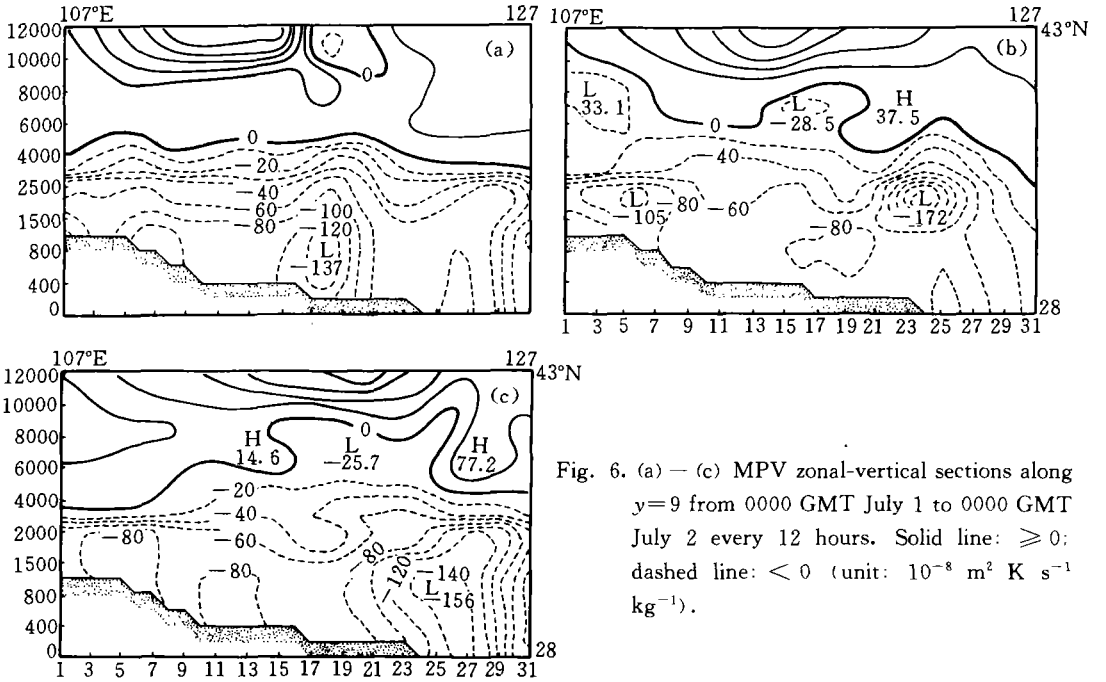

Fig. 6. (a) — (c) MPV zonal-vertical sections along $y=9$ from 0000 GMT July 1 to 0000 GMT July 2 every 12 hours. Solid line: $\geqslant 0$; dashed line: < 0 (unit: 10^{-8} m^2 K s^{-1} kg^{-1}).

decreased in the Changjiang-Huaihe region. On the horizontal figures, it can be seen that the negative MPV center propagated eastward. The center began to intensify again in the Changjiang-Huaihe region at 1200 GMT July 1. By 0000 GMT July 2, another intensive negative MPV area formed in the Changjiang-Huaihe region. And a rainfall center appeared. But its intensity was weaker than that at 0000 GMT July 1. According to the distribution of each term of MPV, absolute vertical vorticity and equivalent potential temperature at 0000 GMT July 2 (figure neglected), it is known that the intensification of negative MPV mainly results from the attribution of the meridional baroclinic effects. Because the stratification in the Changjiang-Huaihe region is neutral, the contribution of $(MPV)_z$ is small. At this time, the precipitation center is excited by the moist symmetric instability produced by $(MPV)_y$.

Finally, Figure 6 depicts the zonal-vertical section of MPV along 32°N ($y=9$) in order to investigate the zonal variation of moist potential vorticity during heavy rain processes. It can be seen that the first rainfall process in the eastern region took place at 118°E ($x=18$) at 0000 GMT July 1 and, 12 hours later, moved eastward to 122°E ($x=26$); simultaneously, the second rainfall process began at 116°E ($x=16$). The negative MPV in the low level and the rainfall corresponding to the latter were weaker than that corresponding to the former. By 0000 GMT July 2, the first process shifted outside the model domain and the second process shifted near $x=27$. From Fig. 6, when convection took place, negative MPV in the low level obviously protruded to the upper troposphere at 10000 m. On the both sides, positive MPV of the upper level can transport downward. Especially at 0000 GMT July 2, the rear positive MPV center appeared below 4000 m. These clearly indicate that the moist potential vorticity structure can well express the characters of the heavy rain processes.

V. CONCLUSIONS

Through above analyses, three conclusions can be reached as follows.

(1) Three-dimensional moist potential vorticity is an important physical variable describing the heavy rain structures and its dynamic mechanisms. The rain belt distributions are well consistent with the low level negative MPV belt distributions. The heavy rain center corresponds the strong negative MPV center. Convections have low level negative MPV transport upward to the upper troposphere and simultaneously have the upper level positive MPV transport downward.

(2) During these heavy rain processes, the contributions of strong negative MPV attribute to the production of the conditional convective instability and the absolute vertical vorticity, as well as the frontal meridional baroclinic effects. The inertial instability in the positive shear vorticity area to the south of the upper level jet also plays a certain role, too. The heavy rain resulting from the Changjiang-Huaihe quasi-stationary front breaking out is always accompanied by the low level jet acceleration. The positive shear vorticity to the north of the jet abruptly increases so that the low level negative MPV center forms.

(3) It is found from this case calculation that the heavy rain process in the Changjiang-Huaihe quasi-stationary front-wind shear line system is affected by not only frontal moist baroclinic effects but also convections, while the heavy rain process in the southwestern region is affected by convective effects.

REFERENCES

Bennits, V. A. and Hoskins, B. J. (1979), Conditional symmetric instability—a possible explanation for frontal rainbands. *Quart. J. Roy. Meteor. Soc.*, **105**: 945—962.

Emanuel, K. A. (1979), Inertial instability and mesoscale convective systems. Part I: linear theory of inertial instability in rotating viscous fluids. *J. Atmos. Sci.*, **36**: 2425—2449.

Hoskins, B. J. (1974), The role of potential vorticity in symmetric stability and instability. *Quart. J. Roy. Meteor. Soc.*, **100**: 480—492.

Reuter, G. W. and Yau, M. K. (1990), Observation of slantwise convective instability in winter cyclones. *Mon. Wea. Rev.*, **118**: 447—458.

Wei Tongjian and Zhang Jing (1995), Diagnosis study of a Meiyu front heavy rain process simulation during summer, 1991. *Meteor. Science*, **15**: 18—26 (in Chinese).

Xu, Q. (1986), Conditional symmetric instability and mesoscale rainbands. *Quart. J. Roy. Meteor. Soc.*, **112**: 315—334.

Zhang Dalin and Cho Hanru (1992), The development of negative moist potential vorticity in squall line. *Mon. Wea. Rev.*, **120**: 1322—1341.